Heliyon 10 (2024) e28672

Contents lists available at ScienceDirect

Heliyon

journal homepage: www.cell.com/heliyon

Research article

Kaempferol-induced mitochondrial damage promotes NF-κB-NLRP3-caspase-1 signaling axis-mediated pyroptosis in gastric cancer cells

Xiafei Qi [a,b,c,1], Jiatong Liu [a,b,c,1], Liuxiang Wang [a,b,c], Peixing Gu [a,b,c], Siyuan Song [a,b,c], Peng Shu [a,b,c,*]

[a] Affiliated Hospital of Nanjing University of Chinese Medicine, Jiangsu, Nanjing, 210029, China
[b] Nanjing University of Chinese Medicine, Jiangsu, Nanjing, 210029, China
[c] Jiangsu Province Hospital of Chinese Medicine, Jiangsu, Nanjing, 210029, China

ARTICLE INFO

Keywords:
Gastric cancer
Kaempferol
Pyroptosis
NLRP3 inflammasome
NF-κB

ABSTRACT

GC is a gastrointestinal tumor with high morbidity and mortality. Owing to the high rate of postoperative recurrence associated with GC, the effectiveness of radiotherapy and chemotherapy may be compromised by the occurrence of severe undesirable side effects. In light of these circumstances, KP, a flavonoid abundantly present in diverse herbal and fruit sources, emerges as a promising therapeutic agent with inherent anti-tumor properties. This study endeavors to demonstrate the therapeutic potential of KP in the context of GC while unraveling the intricate underlying mechanisms. Notably, our investigations unveil that KP stimulation effectively promotes the activation of NLRP3 inflammatory vesicles within AGS cells by engaging the NF-κB signaling pathway. Consequently, the signal cascade triggers the cleavage of Caspase-1, culminating in the liberation of IL-18. Furthermore, we ascertain that KP facilitate AGS cell pyroptosis by inducing mitochondrial damage. Collectively, our findings showcase KP as a compelling candidate for the treatment of GC-related diseases, heralding new possibilities for future therapeutic interventions.

1. Introduction

GC is the third leading cause of cancer-related deaths worldwide [1]. Most patients are diagnosed at advanced stages due to the subtle symptoms of earlier disease and the low rate of regular screening [2]. The coronavirus disease 2019 (COVID-19) pandemic caused delays in the diagnosis and treatment of cancer [3]. Although the impact of the COVID-19 pandemic has gradually diminished, the resumption of healthcare services in its entirety remains incomplete, leaving many advanced-stage patients unable to endure the adverse effects associated with radiation and chemotherapy. Consequently, it is of paramount importance to explore novel approaches for clinical GC treatment through fundamental experiments, providing new insights and directions.

Cellular pyroptosis represents a form of programmed cell death characterized by cellular distension culminating in the rupture of the cell membrane, thereby leading to the release of cellular contents. This process elicits a potent activation of inflammatory and

* Corresponding author. Nanjing University of Chinese Medicine, Jiangsu, Nanjing, 210029, China.
E-mail address: shupengsp@njucm.edu.cn (P. Shu).
[1] Xiafei Qi and Jiatong Liu These authors contributed equally to this work and share the first authorship.

https://doi.org/10.1016/j.heliyon.2024.e28672
Received 5 October 2023; Received in revised form 21 March 2024; Accepted 21 March 2024
Available online 23 March 2024

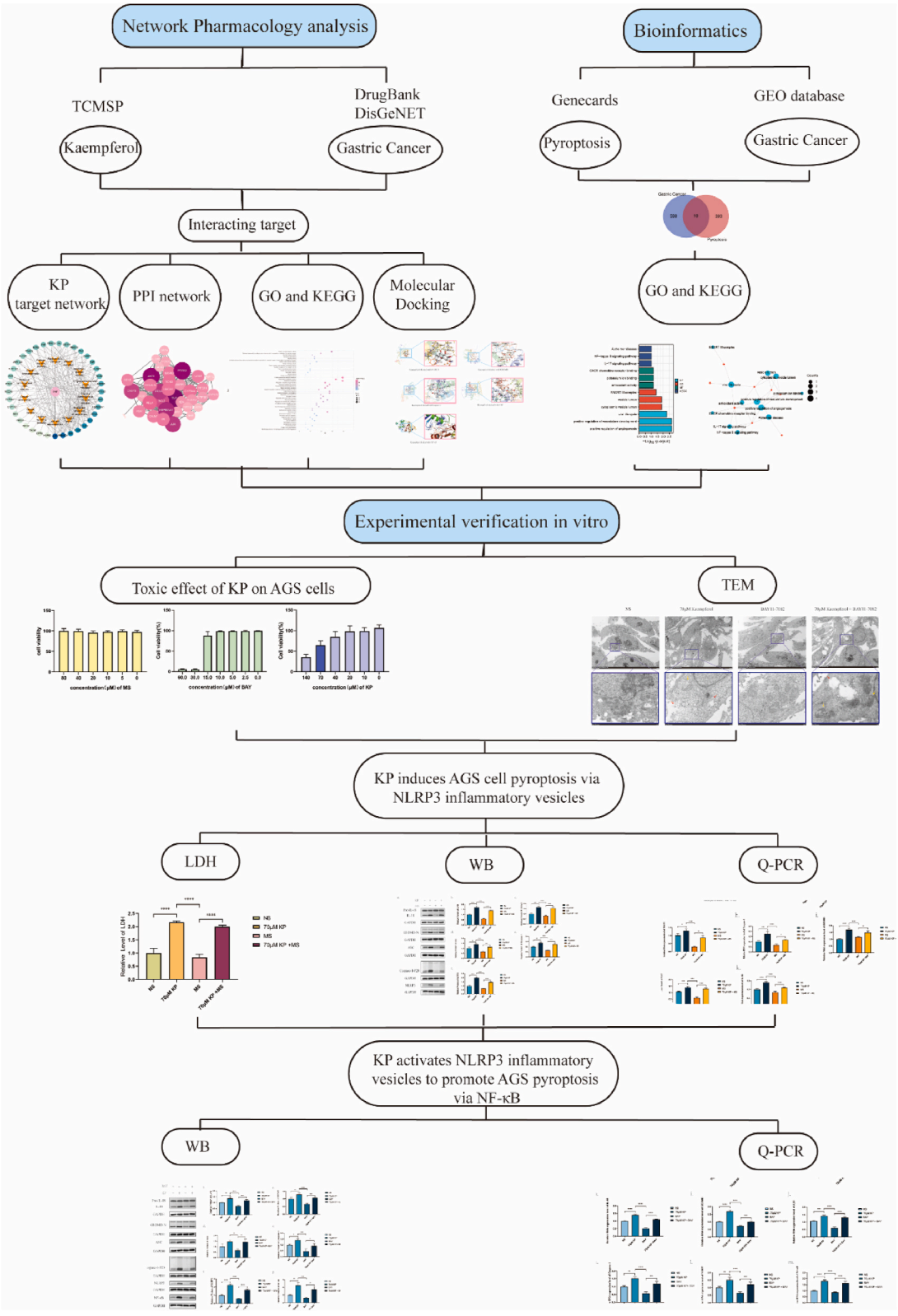

Fig. 1. Technology roadmap for this study.

immune responses [4]. NLRP3 inflammasome, being the most prominent and extensively investigated inflammasome complex, exerts pivotal roles in this context [5]. Activation of NLRP3 triggers the secretion of caspase-1-dependent proinflammatory cytokines IL-1β and IL-18, instigating an inflammatory-related cell death process known as pyroptosis [6].

KP (3,4′,5,7-tetrahydroxyflavone), also known as indigo yellow, represents a nutrient abundantly present in numerous plants, fruits, and vegetables, such as tea, cabbage, broccoli, apples, and grapes [7]. Accumulating scholarly literature substantiates the favorable therapeutic effects of KP on various malignant tumors, including GC [8], lung cancer [9], liver cancer [10], breast cancer [11], and glioma [12].Furthermore, multiple studies have elucidated the anti-cancer potential of KP through various pathways, encompassing inhibition of angiogenesis and vascular endothelial growth factor (VEGF) expression, modulation of hypoxia-inducible factor-1α (HIF-1α)-mediated apoptosis induction, induction of G2/M cell cycle arrest, and caspase-3-dependent cellular apoptosis. Nonetheless, further refinement is warranted to unravel the precise mechanisms underlying the anti-gastric cancer effects of KP [13]. Nonetheless, further refinement is warranted to unravel the precise mechanisms underlying the anti-gastric cancer effects of KP.

In this study, we have demonstrated the robust ability of KP to induce pyroptosis in GC cells. The mechanism underlying this phenomenon involves KP-mediated induction of mitochondrial damage, which subsequently activates the NF-κB signaling pathway, ultimately leading to the activation of the NLPR3-caspase-1 axis and promoting pyroptosis in AGS cells. For specific experimental procedures, please refer to Fig. 1. In light of these findings, it can be concluded that KP, widely present in various fruits and vegetables, exhibits a high level of safety, minimal side effects, superior bioavailability, and potent anti-tumor properties [14]. Consequently, KP holds significant potential as a therapeutic and preventive agent for neoplastic diseases.

2. Materials and methods

2.1. Reagents and materials

KP(Pusi Biotechnology, China)、Dimethyl Dulfoxide(MCE,China)、 CCK8(Yeasen Biotechnology, China)、Anti-Caspase-1 antibody [EPR19672] (ab207802)、Anti-GSDMD antibody[EPR19828] (ab209845)、 Anti-GAPDH antibody [6C5] - Loading Control (ab8245)、 Anti-NLRP3 antibody [EPR23094-1] (ab263899)、 Anti-TMS1/ASC antibody [RM1049] (ab309497)、 Anti-IL-18 antibody [EPR19956] (ab207323)(Abcam.)、 MCC950 Sodium(MS,MCE,China)、 BAY11-7082 (BAY, MCE,China).

2.2. Cell and cultures

AGS(Human gastric adenocarcinoma cells, derived from an untreated gastric adenocarcinoma tissue of a 54-year-old Caucasian woman in 1979,National Collection of Authenticated Cell Cultures, TCHu232) were incubated with 1640 medium (keyGEN BioTECH) containing 10% fetal bovine serum (FBS, abw) with 1% streptomycin-penicillin in an incubator at 37 °C, 5% CO2 level.

2.3. Cell viability assay

Cell viability was assessed to evaluate the responsiveness of cells to KP stimulation, utilizing the CCK8 kit. The AGS cell line was meticulously propagated within 96-well culture plates, with each well being inoculated at an optimal seeding density of 50,000 cells. Upon reaching 80–85% confluence, the culture medium was replaced, and varying concentrations of KP (10 μM/ml, 20 μM/ml, 40 μM/ml, 70 μM/ml, 140 μM/ml) were introduced. After allowing the AGS cells to equilibrate for a full 24 h post-seeding, the culture medium was carefully removed using aspiration. Subsequently, a 10-μL volume of the CCK8 reagent, freshly prepared as a working solution, was added to each well. The plates were then placed in a 37 °C incubator, shielded from light, to facilitate a 2-h incubation period, which is essential for the colorimetric assessment of cell viability. Absorbance measurements (OD) were obtained at a wavelength of 490 nm using a Microplate Reader. The presented data are representative of a minimum of three independent experimental replicates.

2.4. Molecular docking

High-resolution crystal structures of Caspase-1 (ID: 6MFQ, 7AEH), NF-κB (ID: 6P0Z), NLRP3 (ID: 5YQO), GSDMD (ID: 6BZ9), and ASC (ID: 3VLN)were selected from the PDB database, ensuring their structural integrity. Prior to docking simulations, the crystals underwent pretreatment using AutoDock Tools software, which included dehydration and hydrogenation processes. The Autogrid software was employed for the docking simulations, generating binding energies. Visualization and analysis of the obtained results were conducted using pymol software.

2.5. Network pharmacology analysis

The identification of therapeutic targets for KP was accomplished by leveraging the Traditional Chinese Medicine Database and Analysis Platform (TCMSP) [15]. Subsequently, the active targets associated with GC were curated from the DrugBank database [16] and the DisGeNET v6.0 database [17]. The VENNY 2.1.0 Online Interactive Software facilitated the determination of the intersection between the datasets pertaining to KP and disease-related targets. To gain further insights into the functional implications of these identified targets, comprehensive analyses encompassing KEGG, GO-CC, GO-BP, as well as GO-MF were conducted employing the Maspetace database [18].By integrating the comprehensive dataset, a holistic "KP - therapeutic target - pathway of action" diagram was successfully generated, depicting the interplay between KP, its specific targets, and the intricately orchestrated signaling cascades

modulated by this bioactive compound.

2.6. Bioinformatics analysis

The datasets GSE54129 and GSE62254 were obtained from the GEO database using the GEOquery package (v2.54.1) within the R environment (v3.6.3). To ensure data integrity, probes corresponding to multiple molecules were eliminated, with preference given to the probe exhibiting the highest signal value for a particular molecule. Subsequently, the filtered dataset underwent batch-to-batch variation removal utilizing the ComBat function from the sva package (version 3.34.0), considering the distinct datasets as sources of such variation.To gain insights into the sample grouping patterns, principal component analysis (PCA) plots and UMAP plots were generated, enabling the visualization of clustering trends among the different sample groups. Furthermore, leveraging the limma package, differential analyses were performed to identify significant distinctions between the two aforementioned groups.

2.7. TEM analyze

The AGS cells were prepared for analysis following a conventional pre-embedding procedure involving the utilization of agar. Subsequently, the samples were fixed for a duration of 2 h at room temperature, ensuring proper fixation while shielded from light. Following fixation, dehydration and osmotic embedding procedures were employed to prepare the samples for further analysis. To facilitate polymerization, the embedded plates were subjected to an incubation period within an oven set to a controlled temperature of 60 °C, spanning a duration of 48 h. Once the polymerization process was complete, sections were carefully excised from the embedded samples, taking meticulous care to ensure their integrity. Utilizing TEM techniques, performed using an HT7800 instrument manufactured by Hitachi in Japan, each stained section underwent observation and documentation through photographic imaging.

2.8. Western blot

The cells were subjected to a 24-h stimulation with KP, after which they were harvested for protein extraction, enabling the determination of total protein concentration. The extracted proteins underwent separation via electrophoresis using SDS-PAGE gels with varying concentrations of 10%, 12%, and 15%. Post-electrophoresis, proteins were transferred to PVDF membranes for secure immobilization and subsequent analysis in Western blotting. To prevent non-specific binding, the PVDF membrane was blocked and subsequently incubated overnight at 4 °C with specific antibodies, including anti-GAPDH, anti-NLRP3, anti-Caspase-1, anti-GSDMD, anti-IL-18, anti–NF–κB, and anti-ASC. Following a thorough cleansing, the membrane underwent a 2-h incubation at ambient temperature with a secondary antibody, which is essential for the revelation of protein bands previously bound by the primary antibody. Visualization of the protein bands was achieved utilizing a luminescence imaging system, enabling the capture of accurate and reproducible data.

2.9. qRT-PCR analysis

The expression levels of specific target genes via quantitative polymerase chain reaction Q-PCR analysis within this study. The isolation of total RNA was performed utilizing TRNzol regent (TIANGEN, China), a proven reagent renowned for its efficacy in extracting high-quality RNA samples. To facilitate cDNA synthesis, the Reverse Transcription Kit (Vazyme, R323-01), a well-established and reliable kit, was employed.

The relative changes in the expression levels of the target genes were quantified using the 2-ΔΔCt method. To support this analysis, PCR primers were expertly synthesized by Shanghai Sangon Biotech, a well-regarded supplier of molecular biology services based in Shanghai, China.

2.10. LDH release assay

The emission of lactate dehydrogenase (LDH) is a dependable marker for gauging the integrity of cellular membranes and the likelihood of their damage. To measure the quantity of LDH released, an LDH assay kit from the Nanjing Jiancheng Bioengineering Institute in China was utilized. AGS cells were treated with different concentrations of KP(50 μM, 70 μM, and 90 μM) each for a period of 24 h to evaluate their response to the stimulus. In order to evaluate the impact of inhibition, a separate group was pretreated with 20 μM MS for 2 h, followed by subsequent stimulation with different concentrations of KP for 24 h. For each experimental group, cell supernatants were collected and processed according to the instructions provided with the LDH assay kit. Subsequently, the absorbance (OD) of the samples was measured at a wavelength of 450 nm using a Microplate Reader.

2.11. Statistical analysis

The acquired data were obtained from three independent experiments, ensuring reliable and robust statistical analysis. GraphPad Prism 8 software was employed for the statistical analyses conducted in this study. To compare two groups, the independent samples *t*-test was utilized, with a significance level set at $P < 0.05$ to determine statistical significance. To analyze and compare the differences across several groups, a one-way analysis of variance (ANOVA) was conducted, with post-hoc comparisons being made using Tukey's Honestly Significant Difference (HSD) test.

3. Results

3.1. KP elicits mitochondrial damage, thereby facilitating pyroptosis in GC cells

The chemical structure of KP is illustrated in Fig. 2a. The cell viability assay demonstrated (Fig. 2b-d) that GC cells exhibited an IC50 value of 112 μM after 24 h of KP stimulation, leading us to select a working concentration of 70 μM for this study. Microscopic examination (Fig. 2e) revealed distinct observations following 24 h of KP stimulation in AGS cells compared to the control group. Noticeably, the administered group displayed a significant decrease in cell numbers, along with signs of cellular inflammation and swelling. Furthermore, the cells exhibited numerous vacuoles, ruptured cell membranes, and dispersed cellular contents within the culture medium. TEM analysis further corroborated these findings, illustrating ruptured cell membranes and altered cellular morphology, as indicated by the release of cellular contents (highlighted by red arrows). Notably, mitochondrial alterations were also observed, characterized by structural changes, loss of body cristae, internal swelling, and complete loss of structural features in certain mitochondria (indicated by yellow arrows) (Fig. 2f). Collectively, our results elucidate the effective promotion of GC cell pyroptosis by KP, potentially mediated through the induction of mitochondrial damage.

3.2. KP induces the activation of NLRP3 inflammatory vesicles, leading to the induction of pyroptosis

Pyroptosis, an inflammatory form of necrosis, is characterized by the activation of the NLRP3 inflammasome, followed by downstream caspase-1 activation, ultimately resulting in the release of the inflammatory factor IL-18 [19]. The conversion of the NLRP3 protein from a dormant homogenous oligomeric complex to an activated form marks the initiation of a cascade within the inflammasome pathway. This process prompts the structural reorganization of the ASC adaptor protein into a helical oligomeric configuration. This newly formed ASC assembly acts as a scaffold, facilitating the activation of caspase-1, a key enzyme in the maturation and release of inflammatory cytokines [20]. Notably, several studies have demonstrated the regulatory role of KP in NLRP3 activation in various diseases, highlighting its potential for preventive and therapeutic interventions [21–24].To investigate the impact of KP on NLRP3 inflammasome activation, we initially conducted molecular docking simulations to predict the binding sites between KP and key molecules such as NLRP3, GSDMD, Caspase-1, ASC, and NF-κB (Fig. 3a–e). The results revealed that KP exhibited the strongest binding energy with NLRP3 (−8.7 kJ), followed by ASC (−7.4 kJ) and Caspase-1 (−8.1 kJ). Lower docking energy indicates a more stable binding conformation between the protein ligand and the drug molecule. Based on these findings, we postulated that KP-induced NLRP3 activation led to Caspase-1 cleavage, thereby promoting pyroptosis in GC cells.

Subsequently, we assessed the release of LDH, a major product released during pyroptosis, in AGS cells stimulated with KP. Remarkably, LDH release significantly increased upon KP stimulation. Furthermore, the inhibitory effect of MS on LDH release was counteracted by KP (Fig. 3f). We then evaluated the activation levels of NLRP3 and Caspase-1 in the administered group and MS group

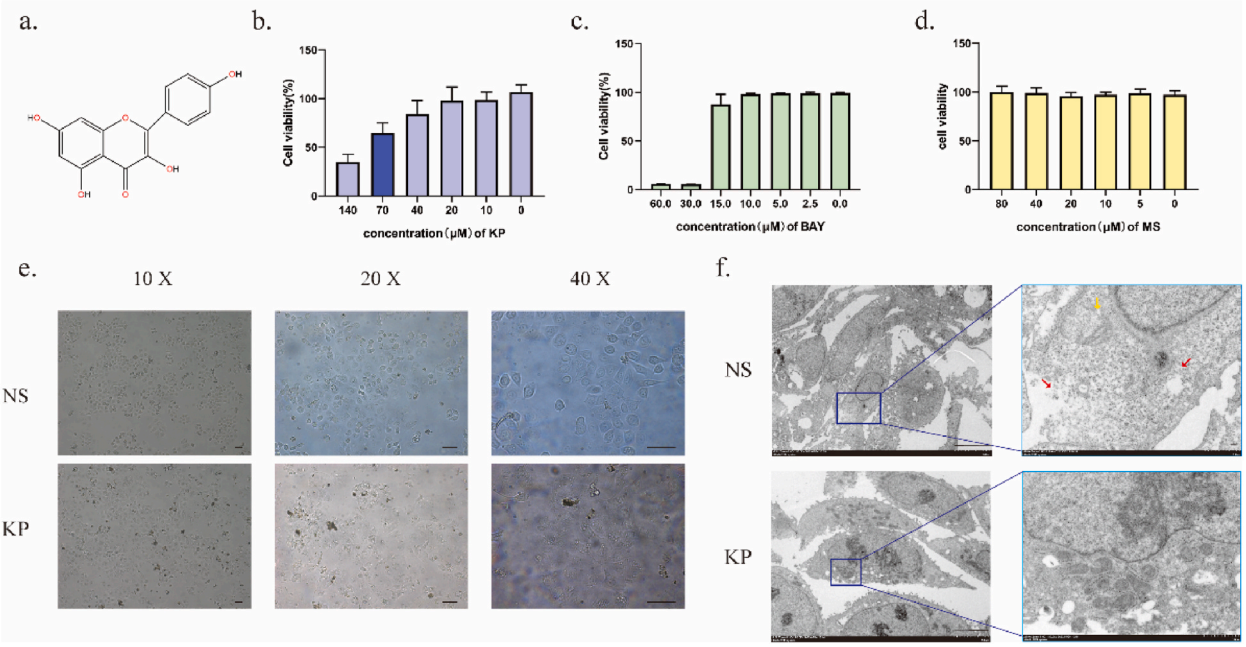

Fig. 2. Promotion of AGS cell pyroptosis by KP. a. Chemical structure of KP. b-d. IC50 values of AGS cells under various drug stimuli, including KP, BAY, and MS. e. Microscopic examination depicting the morphological alterations of AGS cells at different magnifications (10×, 20X, 40X). f. TEM images illustrating the changes in AGS cell morphology. Red arrows indicate AGS cell membrane rupture, while yellow arrows highlight AGS cell mitochondrial changes. (For interpretation of the references to color in this figure legend, the reader is referred to the Web version of this article.)

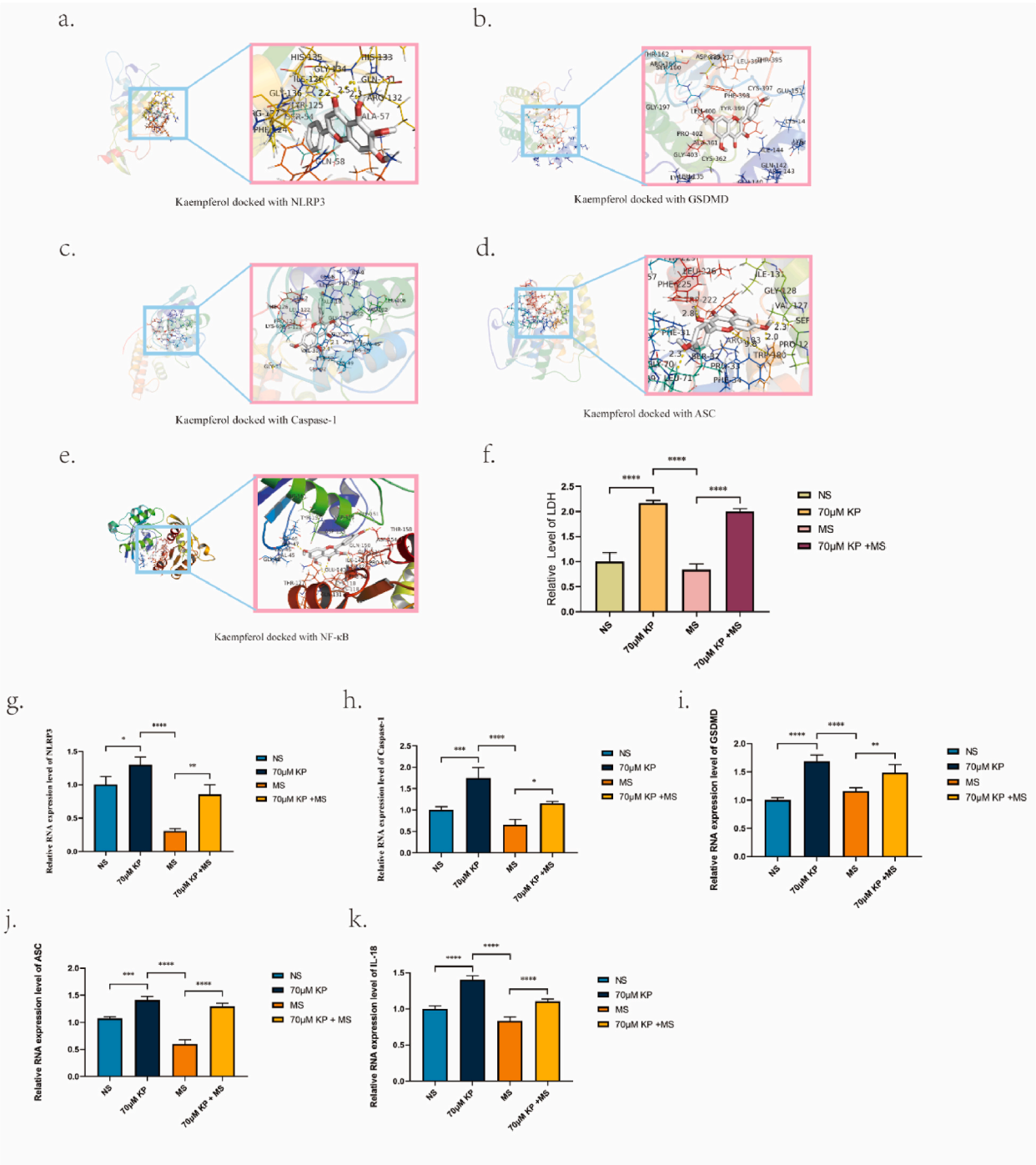

Fig. 3. The pivotal role played by KP in activating NLRP3 inflammatory vesicles, thereby inducing pyroptosis in GC cells. a-e. Molecular docking simulations depicting the interaction between KP and key molecules involved in pyroptosis, including NLRP3, GSDMD, Caspase-1, ASC, and NF-κB. f. Quantification of LDH release from AGS cells following stimulation with KP. g-k. Analysis of mRNA expression levels for NLRP3, Caspase-1, GSDMD, ASC, and IL-18 in AGS cells treated with pharmacological agents.

cells using immunoblotting and PCR techniques. The PCR results indicated that KP promoted the activation of NLRP3 in AGS cells (Fig. 3g), subsequently activating Caspase-1 (Fig. 3h) and releasing the active N-terminus of GSDMD (Fig. 3i). Additionally, KP upregulated the level of ASC (Fig. 3j) and facilitated the secretion of IL-18 (Fig. 3k). Collectively, these findings highlight the ability of KP to induce NLRP3 inflammasome activation, resulting in caspase-1 cleavage and subsequent pyroptosis in GC cells.

In the WB results, it can also be observed that KP exhibited a mitigating effect on the inhibitory actions of MS regarding the

expression levels of NLRP3 (Fig. 4a and f), Caspase-1 (Fig. 4a and e), GSDMD(Fig. 4a,c)ASC (Fig. 4a and d), and IL-18 (Fig. 4a and b).

This information highlights that KP counteracted the inhibitory effects of MS on the expression of key pyroptosis-related molecules, such as Caspase-1, GSDMD, ASC, and IL-18. This evidence demonstrates that KP promotes pyroptosis in AGS cells in close association with the NLRP3 inflammasome. Additionally, the agreement between WB, and qPCR results reinforces the reliability and consistency of our experimental observations.

3.3. KP facilitates pyroptosis via modulation of the NF-κB-NLRP3-caspase-1 signaling axis

The activation of the NF-κB signaling pathway plays a critical role in initiating inflammasome assembly and subsequently triggering pyroptosis [25]. Notably, this classical inflammatory pathway is closely linked to the activation of the NLRP3 inflammasome [26]. In order to investigate the impact of KP on NF-κB activation, we employed bioinformatics analyses (Fig. 5a–c), network pharmacology approaches (Fig. 5d–f, Fig. 6), as well as molecular docking predictions to guide our subsequent experimental investigations. The results obtained from these preliminary analyses have revealed that NF-κB serves as a pivotal pathway connecting GC and pyroptosis. Furthermore, through interaction analysis with KP's target molecules, we identified that KP specifically acts on the pyroptosis-related targets within GC cells. Notably, our findings indicate a strong docking affinity between KP and the RELA protein, which is a classical component of the NF-κB pathway. Our initial investigations suggest that KP may exert its effects on cellular pyroptosis in GC cells through the modulation of the NF-κB-NLRP3-Caspase-1 signaling axis.

Furthermore, through Microscopic examination (Fig. 7a) and TEM analysis (Fig. 7b), we observed that KP induced notable cellular abnormalities, including cell membrane rupture and mitochondrial alterations. Intriguingly, these morphological changes were substantially attenuated when co-treated with BAY, a specific inhibitor of NF-κB signaling. Conversely, AGS cells stimulated solely with BAY exhibited no discernible morphological alterations. These findings provide compelling evidence supporting the significance of NF-κB as a crucial target in mediating KP-induced promotion of pyroptosis.

To further corroborate the impact of KP on the NF-κB signaling pathway, we conducted WB and qPCR analyses to assess the expression levels of key molecules involved. Specifically, we examined the protein and mRNA levels of NF-κB P65, NLRP3, Caspase-1, ASC, GSDMD, and IL-18 in each experimental group. The results demonstrated a significant upregulation of NF-κB, NLRP3, Caspase-1, ASC, GSDMD, and IL-18 at the protein (Fig. 8a–g)and mRNA (Fig. 8h-m)levels upon KP treatment. Moreover, when AGS cells were pretreated with BAY, an inhibitor of NF-κB signaling, KP effectively counteracted the inhibitory effects on NLRP3, Caspase-1, ASC,

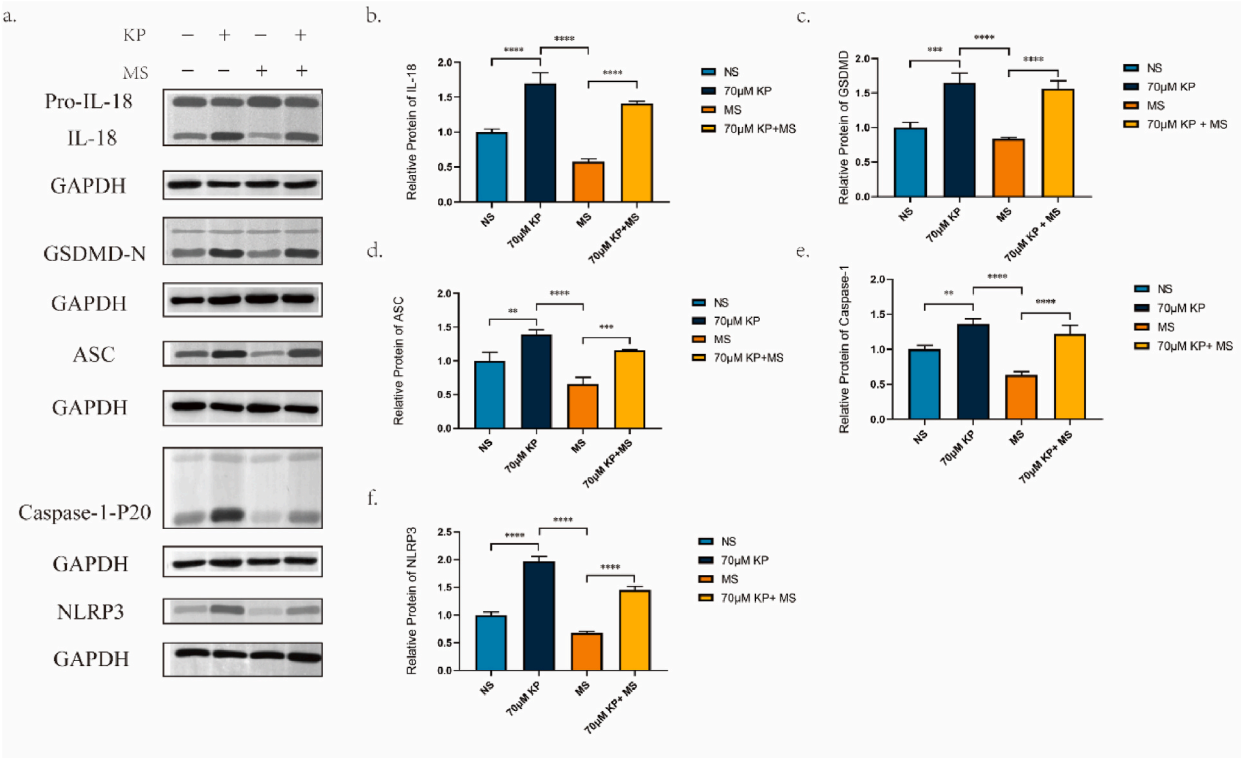

Fig. 4. The impact of KP on the expression levels of key pyroptosis-related pathway proteins in AGS cells. a. Protein banding diagrams showing the expression levels of IL-18, GSDMD-N, ASC, Caspase-1, and NLRP3. Fig. 1 in Appendix 1 provides the full, non-adjusted Western Blot images(1-1: IL-18, 1–2: GSDMD-N, 1–3: ASC, 1–4: Caspase-1, 1–5: NLRP3). b-f. Results of banding analysis representing the expression levels of IL-18, GSDMD-N, ASC, Caspase-1, and NLRP3.

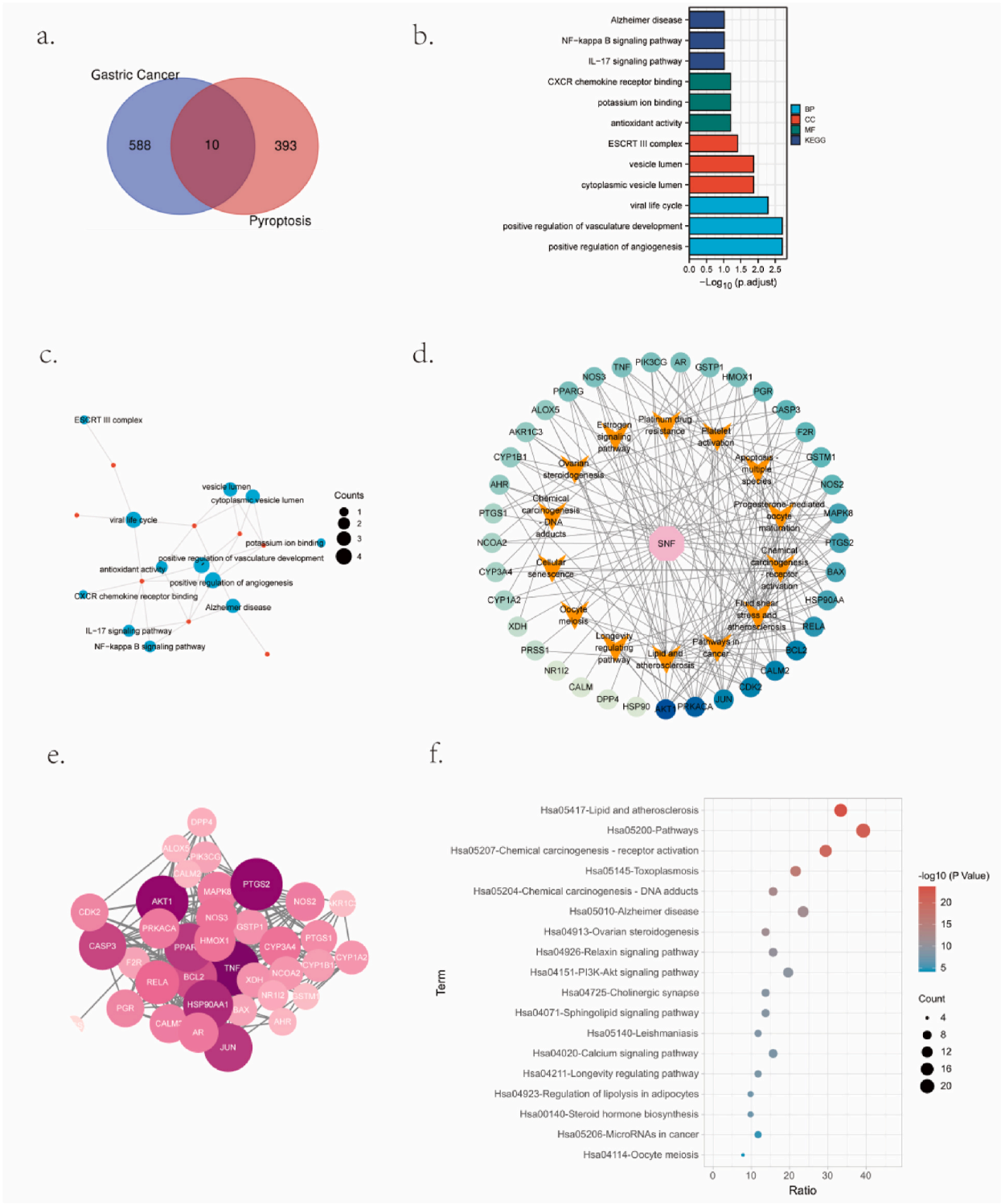

Fig. 5. Comprehensive bioinformatics analyses exploring the intricate relationships between KP, GC, and pyroptosis. a. Identification of interacting genes linking GC and pyroptosis. b. KEGG pathway analysis depicting the functional and regulatory pathways associated with the interacting genes involved in GC and pyroptosis. c. Network diagram illustrating the interconnections among the KEGG pathways identified in GC and pyroptosis. d. Network diagram revealing the target-pathway network of KP in GC. e. Protein-protein interaction (PPI) map showcasing the genes implicated in KP's action within GC. f. Analysis of KP's influence on the KEGG pathway of GC-related genes.

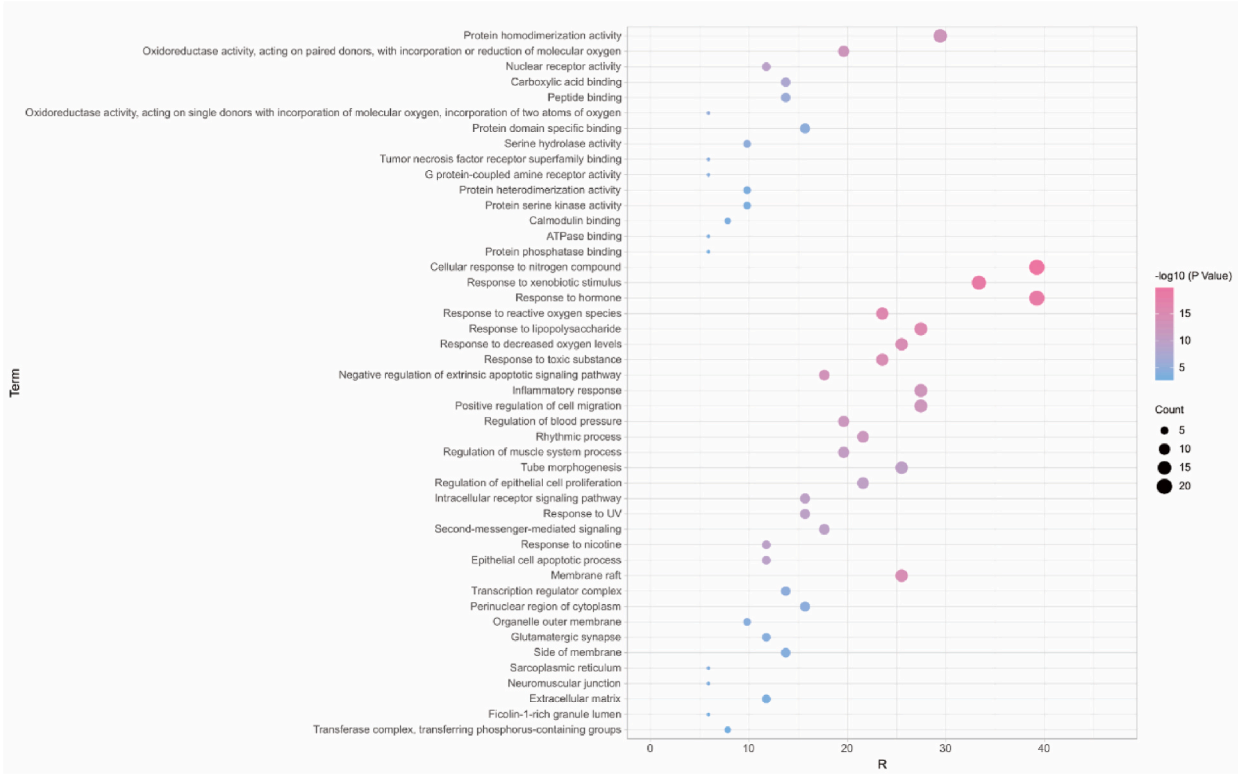

Fig. 6. Gene GO analysis of KP action in gastric cancer.

GSDMD, and IL-18 expression, displaying an observable trend of upregulation. These findings provide strong evidence for the involvement of KP in modulating the NF-κB signaling pathway. The upregulation of NF-κB, NLRP3, Caspase-1, ASC, GSDMD, and IL-18 at both the protein and mRNA levels further supports the role of KP in promoting pyroptosis-related processes. Additionally, the antagonistic effect of KP against the inhibitory action of BAY highlights its ability to override the suppressive effects on the expression of critical pyroptotic molecules.

4. Discussions

GC is a prevalent gastrointestinal tumor associated with high morbidity and mortality rates [27]. Conventional treatment strategies for GC encompass surgical interventions, radiotherapy, and chemotherapy. However, the efficacy of these approaches may be compromised due to postoperative recurrence and severe adverse effects associated with radiotherapy and chemotherapy [28]. Consequently, there is growing interest in exploring alternative therapies with reduced side effects, such as traditional herbal medicines and their constituent compounds.

KP, a natural flavonoid commonly found in traditional herbal medicine, has attracted attention for its anticancer properties [29]. Given its therapeutic potential, our research team aims to investigate the underlying anti-tumor mechanisms of KP. Among various factors influencing GC progression, cell death holds significant importance [27]. Pyroptosis, an inflammatory programmed cell death process, is pivotal in the initiation of tumors, the advancement of various diseases, and the facilitation of cancer spread and metastasis [30].

In our study, we sought to explore the relationship between KP, GC, and pyroptosis. By conducting TEM observations, we confirmed that KP-induced cell death in GC cells exhibited characteristic features of pyroptosis. Additionally, morphological alterations in mitochondria suggested that KP may promote pyroptosis by inducing mitochondrial damage.

The NLRP3 inflammasome comprises three key components: the sensor NLRP3, adaptor ASC, and effector caspase-1 [31]. To investigate the impact of KP on NLRP3 inflammasome activation, we assessed intracellular levels of NLRP3, caspase-1, ASC, and IL-18 using WB and Q-PCR. Our findings demonstrated that KP indeed facilitates pyroptosis in AGS cells through the NLRP3-Caspase-1 axis.

Based on our experimental results, we employed bioinformatics, network pharmacology, and molecular docking analyses to predict that KP activates the NLRP3 inflammasome via the NF-κB signaling pathway. This activation leads to the cleavage of downstream effector Caspase-1 and subsequent release of the proinflammatory cytokine IL-18. Through TEM observation, WB, and qPCR, we examined the levels of NF-κB, NLRP3, Caspase-1, ASC, GSDMD, and IL-18 proteins and mRNA in the blank group, drug group, BAY group, and drug combined with BAY group, confirming that the NLRP3-Caspase-1 axis is activated by the NF-κB signaling pathway. However, this study inevitably has some limitations. Firstly, the drug targets and genes obtained from bioinformatics and network

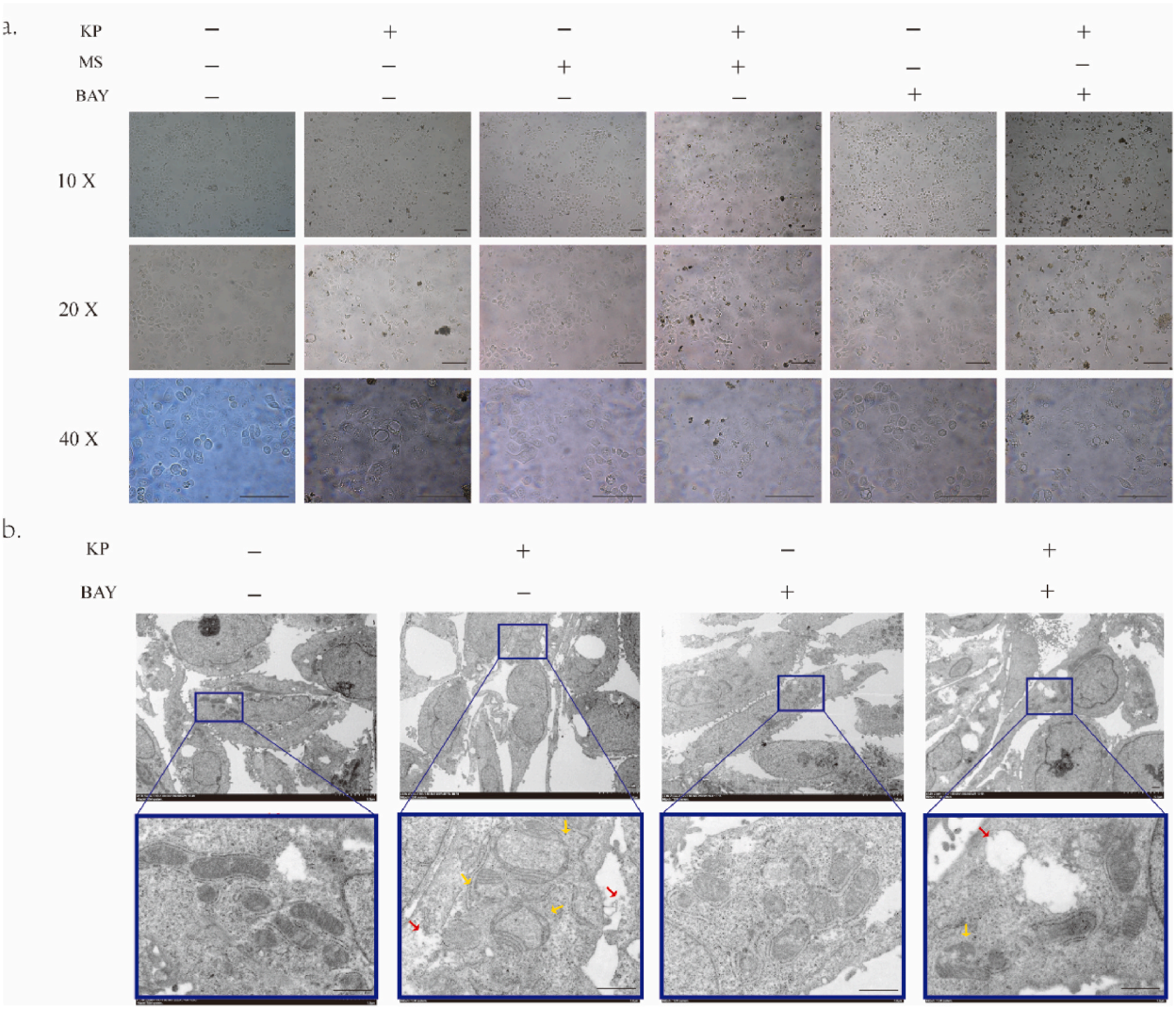

Fig. 7. Morphological modifications occurring in AGS cells upon stimulation with KP. a. Visualization of morphological changes in AGS cells using an inverted fluorescence microscope. b. Morphological alterations in AGS cells observed through TEM.

pharmacology databases have certain limitations. Secondly, we only conducted basic experiments and did not extend the conclusions to clinical trials for validation. Lastly, the "evidence chain" regarding KP-induced mitochondrial damage leading to pyroptosis in GC cells requires further refinement.

5. Conclusion

KP may promote pyroptosis in GC cells by inducing mitochondrial damage and activating the NF-κB-NLRP3-caspase-1 signaling axis. The promotion of pyroptosis may represent one of the potential mechanisms underlying KP's anti-tumor effects. Further in-depth investigation into the mechanism of KP in treating GC can aid in the identification of valuable cancer treatment modalities.

Abbreviations list

Full Name	Abridge
Gastric cancer	GC
Kaempferol	KP
Transmission Electron Microscope	TEM
Western blot	WB

(*continued on next page*)

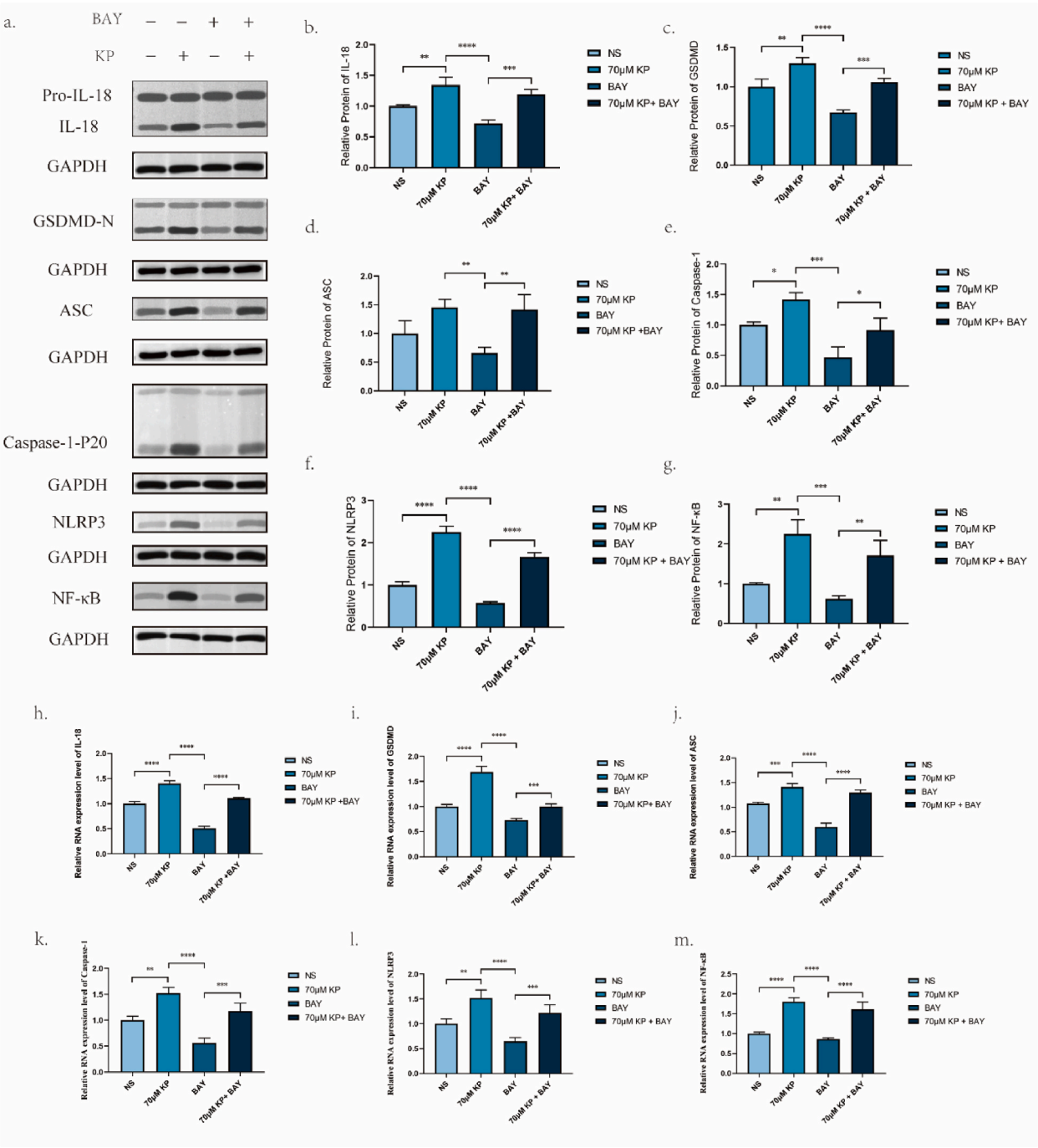

Fig. 8. Expression Levels of NF-κB P65, NLRP3, GSDMD, Caspase-1, ASC and IL-18 in AGS Cells. Appendix 1 a. WB bands depicting the expression of NF-κB P65, NLRP3, GSDMD, Caspase-1, ASC and IL-18 in AGS cells. Fig. 2 in Appendix 1 provides the full, non-adjusted Western Blot images(2-1: IL-18, 2-2: GSDMD-N, 2–3: ASC, 2–4: Caspase-1, 2–5: NLRP3, 2–6: NF-κB). b-g. Protein expression results showcasing the levels of NF-κB P65, NLRP3, GSDMD, Caspase-1, ASC and IL-18 in AGS cells. h-m. Results of mRNA expression analysis indicating the levels of NF-κB P65, NLRP3, GSDMD, Caspase-1, ASC and IL-18 in AGS cells.

(*continued*)

Full Name	Abridge
Quantitative real-time PCR analysis	PCR
Lactate dehydrogenase	LDH

Funding

This work was funded by the National Natural Science Foundation of China (nos. 82374539). Key projects of the Jiangsu Province Traditional Chinese Medicine Science and Technology Development Plan (ZD202214).

Ethical considerations

The cell lines utilized in this study were of human origin and were acquired from the National Collection of Authenticated Cell Cultures.

This study did not require review and/or approval from an ethics committee, as it did not involve research within human or animal subjects or clinical cases.

Data availability statement

Datasets of gastric cancer targets generated during this study are available in DrugBank database and the DisGeNET database repository, [DrugBank database: https://go.drugbank.com/]. [DisGeNET database: https://www.disgenet.org].The dataset of baicalein targets generated during this study is available in the TCMSP database, [https://tcmsp-e.com/].Datasets of Pyroptosis targets generated during this study are available in Genecards database. [Genecards: https://www.genecards.org/cgi-bin/carddisp.pl?gene=%s]. Datasets of gastric cancer targets of humon generated during this study are available in GEO database. [GEO database: https://www.ncbi.nlm.nih.gov/gds]. The intersection between the datasets related to KP and disease-associated targets in this study was determined using the VENNY 2.1.0 online interactive software.[https://bioinfogp.cnb.csic.es/tools/venny/].

CRediT authorship contribution statement

Xiafei Qi: Writing – original draft, Data curation. **Jiatong Liu:** Visualization, Investigation, Data curation. **Liuxiang Wang:** Methodology, Formal analysis. **Peixing Gu:** Supervision, Software. **Siyuan Song:** Methodology. **Peng Shu:** Writing – review & editing, Conceptualization.

Declaration of generative AI and AI-assisted technologies in the writing process

During the preparation of this work the author(s) used chatgpt in order to improve language and readability. After using this tool/service, the author(s) reviewed and edited the content as needed and take(s) full responsibility for the content of the publication.

Declaration of competing interest

The authors declare that they have no known competing financial interests or personal relationships that could have appeared to influence the work reported in this paper.

Appendix A. Supplementary data

Supplementary data to this article can be found online at https://doi.org/10.1016/j.heliyon.2024.e28672.

References

[1] J.A. Ajani, et al., Gastric cancer, version 2.2022, NCCN clinical practice guidelines in oncology, J. Natl. Compr. Cancer Netw. 20 (2) (2022) 167–192.
[2] W.-L. Guan, Y. He, R.-H. Xu, Gastric cancer treatment: recent progress and future perspectives, J. Hematol. Oncol. 16 (1) (2023).
[3] R.L. Siegel, et al., Cancer statistics, 2023, Ca-Cancer J. Clin. 73 (1) (2023) 17–48.
[4] X. Wei, et al., Role of pyroptosis in inflammation and cancer, Cell. Mol. Immunol. 19 (9) (2022) 971–992.
[5] X. Lv, et al., Isoliquiritigenin alleviates P. gingivalis-LPS/ATP-induced pyroptosis by inhibiting NF-κB/NLRP3/GSDMD signals in human gingival fibroblasts, Int. Immunopharm. 101 (Pt B) (2021) 108338.
[6] Y.Y. Chen, et al., Skin damage induced by zinc oxide nanoparticles combined with UVB is mediated by activating cell pyroptosis via the NLRP3 inflammasome-autophagy-exosomal pathway, Part. Fibre Toxicol. 19 (1) (2022) 2.
[7] R. Kubina, et al., Kaempferol and fisetin-related signaling pathways induce apoptosis in head and neck cancer cells, Cells 12 (12) (2023).
[8] J. Ren, et al., Recent progress regarding kaempferol for the treatment of various diseases, Exp. Ther. Med. 18 (4) (2019) 2759–2776.
[9] E. Jo, et al., Kaempferol suppresses transforming growth factor-β1-induced epithelial-to-mesenchymal transition and migration of A549 lung cancer cells by inhibiting akt1-mediated phosphorylation of Smad3 at threonine-179, Neoplasia 17 (7) (2015) 525–537.
[10] F. Tie, et al., Kaempferol and kaempferide attenuate oleic acid-induced lipid accumulation and oxidative stress in HepG2 cells, Int. J. Mol. Sci. 22 (16) (2021).
[11] R.K. Sindhu, et al., Impacting the remedial potential of nano delivery-based flavonoids for breast cancer treatment, Molecules 26 (17) (2021).
[12] M. Chen, et al., Kaempferol inhibits non-homologous end joining repair via regulating Ku80 stability in glioma cancer, Phytomedicine 116 (2023) 154876.

[13] A. Almatroudi, et al., Effects and mechanisms of kaempferol in the management of cancers through modulation of inflammation and signal transduction pathways, Int. J. Mol. Sci. 24 (10) (2023).
[14] T. Lomphithak, et al., Natural flavonoids quercetin and kaempferol targeting G2/M cell cycle-related genes and synergize with smac mimetic LCL-161 to induce necroptosis in cholangiocarcinoma cells, Nutrients 15 (14) (2023).
[15] J. Ru, et al., TCMSP: a database of systems pharmacology for drug discovery from herbal medicines, J. Cheminf. 6 (2014) 13.
[16] D.S. Wishart, et al., DrugBank 5.0: a major update to the DrugBank database for 2018, Nucleic Acids Res. 46 (D1) (2018) D1074–d1082.
[17] J. Piñero, et al., The DisGeNET knowledge platform for disease genomics: 2019 update, Nucleic Acids Res. 48 (D1) (2020) D845–d855.
[18] Y. Zhou, et al., Metascape provides a biologist-oriented resource for the analysis of systems-level datasets, Nat. Commun. 10 (1) (2019) 1523.
[19] A. Al Mamun, et al., Pyroptosis in acute pancreatitis and its therapeutic regulation, Apoptosis 27 (7–8) (2022) 465–481.
[20] A. Akbal, et al., How location and cellular signaling combine to activate the NLRP3 inflammasome, Cell. Mol. Immunol. 19 (11) (2022) 1201–1214.
[21] X. Han, et al., Small molecule-driven NLRP3 inflammation inhibition via interplay between ubiquitination and autophagy: implications for Parkinson disease, Autophagy 15 (11) (2019) 1860–1881.
[22] Z. Liu, et al., Pretreatment with kaempferol attenuates microglia-mediate neuroinflammation by inhibiting MAPKs?NF??B signaling pathway and pyroptosis after secondary spinal cord injury, Free Radic. Biol. Med. 168 (2021) 142–154.
[23] H. Lim, et al., Flavonoids interfere with NLRP3 inflammasome activation, Toxicol. Appl. Pharmacol. 355 (2018) 93–102.
[24] C. Ling, et al., Kaempferol attenuates retinal ganglion cell death by suppressing NLRP1/NLRP3 inflammasomes and caspase-8 via JNK and NF-kappa B pathways in acute glaucoma, Eye 33 (5) (2019) 777–784.
[25] Y. Tan, et al., Tumor suppressor DRD2 facilitates M1 macrophages and restricts NF-κB signaling to trigger pyroptosis in breast cancer, Theranostics 11 (11) (2021) 5214–5231.
[26] A. Li, et al., GATA6 promotes fibrotic repair of tracheal injury through NLRP3 inflammasome-mediated epithelial pyroptosis, Int. Immunopharm. 123 (2023) 110657.
[27] H. Wang, et al., Cell death affecting the progression of gastric cancer, Cell Death Dis. 8 (1) (2022) 377.
[28] Y. Fan, et al., Curcumin against gastrointestinal cancer: a review of the pharmacological mechanisms underlying its antitumor activity, Front. Pharmacol. 13 (2022) 990475.
[29] T.W. Kim, et al., Kaempferol induces autophagic cell death via IRE1-JNK-CHOP pathway and inhibition of G9a in gastric cancer cells, Cell Death Dis. 9 (9) (2018) 875.
[30] N. Zaffaroni, G.L. Beretta, The therapeutic potential of pyroptosis in melanoma, Int. J. Mol. Sci. 24 (2) (2023).
[31] J. Fu, H. Wu, Structural mechanisms of NLRP3 inflammasome assembly and activation, Annu. Rev. Immunol. 41 (2023) 301–316.